



Opinion: Eliminating aircraft soot emissions

Una Trivanovic and Sotiris E. Pratsinis

Particle Technology Laboratory, Department of Mechanical and Process Engineering, ETH Zürich,
8092, Switzerland

Correspondence to: Sotiris E. Pratsinis (sotiris.pratsinis@ptl.mavt.ethz.ch)

1 Abstract

2 Soot from aircraft engines deteriorates air quality around airports and can contribute to climate change primarily
3 by influencing cloud processes and contrail formation. Simultaneously, aircraft engines emit CO₂, nitrogen
4 oxides (NO_x) and other pollutants which also negatively affect human health and the environment. While urgent
5 action is needed to reduce all pollutants, strategies to reduce one pollutant may increase another, calling for a
6 need to decrease, for example, the uncertainty associated with soot's contribution to net Radiative Forcing (RF)
7 in order to design targeted policies that minimize the formation and release of all pollutants. Aircraft soot is
8 characterized by rather small median mobility diameters, $d_m = 8 - 60$ nm, and at high thrust, low (< 25%)
9 organic carbon to total carbon (OC/TC) ratios while at low thrust the OC/TC can be quite high. Computational
10 models could aid in the design of new aircraft combustors to reduce emissions, but current models struggle to
11 capture the soot d_m , and volume fraction, f_v measured experimentally. This may be in part due to
12 oversimplification of soot's irregular morphology in models and a still poor understanding of soot inception.
13 Nonetheless, combustor design can significantly reduce soot emissions through extensive oxidation or near-
14 premixed, lean combustion. For example, lean premixed prevaporized combustors significantly reduce emissions
15 at high thrust by allowing injected fuel to fully vaporize before ignition while low temperatures from very lean
16 jet fuel combustion limit the formation of NO_x. Alternative fuels can be used alongside improved combustor
17 technologies to reduce soot emissions. However, current policies and low supply promote the blending of
18 alternative fuels at low ratios (~1%) for all flights, rather than using high ratios (> 30%) in a few flights which
19 could meaningfully reduce soot emissions. Here, existing technologies for reducing such emissions through
20 combustor and fuel design will be reviewed to identify strategies that eliminate them.

21 1. Introduction

22 Aviation is a growing industry with a significant impact on human health and the environment due to the
23 emission of combustion by-products, including soot aerosols. The latter is one of the most important contributors
24 to climate change (Bond et al., 2013) and a component of air pollution known to cause cancer, cardiovascular
25 and respiratory diseases, and it has been correlated with various other illnesses (Niranjan and Thakur, 2017).
26 Regulations around the world have been limiting soot emissions since the 1970s. The International Civil
27 Aviation Organization (ICAO) until recently limited only the 'smoke number', essentially visible black smoke
28 from aircraft engines which caused dangerous reductions in visibility around airports (George et al., 1972).
29 Modern engines have no visible smoke but still produce invisible nanoparticles (Durdina et al., 2017). In 2020,
30 smoke number was replaced with a limit on the mass concentration of non-volatile Particulate Matter (nvPM)
31 and in 2023 an additional limit was placed on the number concentration of nvPM for all new engines with a rated
32 thrust greater than 26.7 kN (ICAO, 2017). Thus, jet engine manufacturers must design new engines to meet the
33 new nvPM standards without exceeding the regulations limiting nitrogen oxides (NO_x), unburned hydrocarbons
34 (UHC) or carbon monoxide (CO) emissions while still maintaining strict safety standards. These regulations are
35 aimed at improving local air quality, so engines are assessed based on a standardized landing and take-off (LTO)
36 cycle most relevant for emissions near the ground.

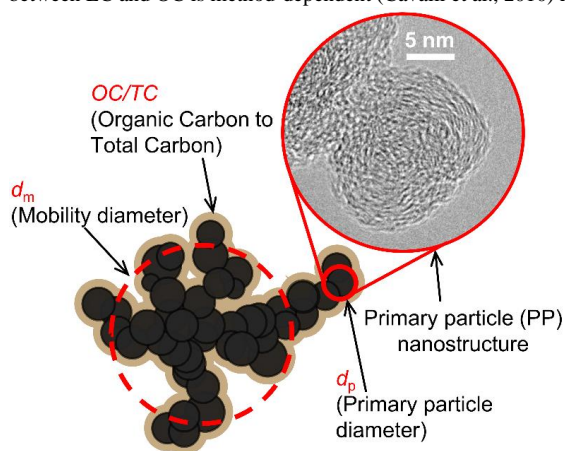
37 Soot emissions can impact the climate by warming the atmosphere through direct Radiative Forcing
38 (RF) and indirectly by altering cloud processes and decreasing snow albedo (Bond et al., 2013). Aviation is
39 unique in that it emits soot at high altitude with very different atmospheric conditions (e.g., temperature and
40 pressure) from those on the ground. This may influence the formation of contrails (Kärcher, 2018). Lee et al.
41 (2021) estimated the climate forcing contribution of CO₂, contrail cirrus, NO_x, soot aerosols, SO₂ aerosols and
42 water vapor from aviation in 2018. By these estimates, contrails account for 57.4 mWm⁻² or 55% of aviation's
43 net radiative forcing but with 95% confidence intervals from 27 – 67% of the net RF illustrating the high
44 uncertainty. The exact RF of contrail cirrus depends on the atmospheric conditions along the flight track and
45 time of day. At night, contrails have an exclusively warming effect while during the day there can be a warming
46 and a cooling effect (Stuber et al., 2006).



47 The estimate of direct RF from soot was relatively low, 0.9 mWm^{-2} (Lee et al., 2021). However,
48 inventories of global soot emissions from aircraft can vary by two orders of magnitude (Agarwal et al., 2019).
49 Present inventories are based on the LTO cycle which focuses on landing and take-off at sea-level rather than
50 high-altitude cruise. As these emissions are measured only at ground level for the LTO cycle, the emissions most
51 relevant for climate considerations are only indirectly estimated (Stettler et al., 2013). In addition, the LTO cycle
52 does not exactly match the real time at each thrust for example, the LTO cycle assumes idle/taxi is 7% but real
53 aircraft use between 3 – 17% thrust for these conditions. (Masiol and Harrison, 2014). Estimates of the RF of
54 soot are from climate models which may underestimate the contribution of soot (Kelesidis et al., 2022). While
55 CO_2 remains in the atmosphere for 100 years or more, soot and contrails have short atmospheric lifetimes on the
56 order of a week (Bond et al., 2013) or hours (Bock and Burkhardt, 2016), respectively, so their global warming
57 potential is most important in the short term. This presents an opportunity to make immediate reductions in
58 global warming and ‘buying time’ for the implementation of technologies to lower CO_2 emissions (Montzka et
59 al., 2011). This may be important for the aviation industry which in 2022, adopted an ambitious goal of net-zero
60 carbon emissions by 2050.

61 These uncertainties highlight the importance of further research to better quantify the role of soot in
62 both contrail formation (Marcolli et al., 2021) and direct radiative forcing (Kelesidis et al., 2022). Such
63 uncertainties make it difficult to accurately assess priorities in emission reductions as there are often trade-offs
64 between emissions. For example, reductions in soot often result in an increase in NO_x from diesel engines (Kim
65 et al., 2009). Similarly, contrail formation can be avoided by diverting flights to airspace with unfavorable
66 conditions for contrail formation (e.g. warmer temperatures) but may result in higher fuel consumption and, thus,
67 CO_2 emissions (Teoh et al., 2020). The large uncertainty associated with the contribution of soot to climate
68 change is in part due to the oversimplification of soot morphology in climate models which typically assume
69 soot to be coated spheres. In reality, soot is an agglomerate composed of polydisperse primary particles (PP),
70 illustrated in Figure 1, with a nanostructure of layered graphene sheets (Fig. 1: inset).

71 The relative amounts of Organic Carbon (OC) or Elemental Carbon (EC) compared to the Total Carbon
72 (TC) is typically used to quantify the chemical composition of the particles. The OC is
73 defined by the ICAO as “...carbon volatilized in Helium while heating a quartz fiber filter sample to $870 \text{ }^\circ\text{C}$
74 during thermal optical transmittance analysis including char formed during pyrolysis of some materials”.
75 Conversely, EC is “...light absorbing carbon that is not removed from a filter sample heated to $870 \text{ }^\circ\text{C}$ in an inert
76 atmosphere during thermal optical transmittance analysis, excluding char” (ICAO, 2017). So, while quantifying
77 OC/EC ratios is important for understanding the light absorption of soot (Kelesidis et al., 2021), the split
78 between EC and OC is method-dependent (Cavalli et al., 2010) rather than a discrete property.



79
80 **Figure 1:** A schematic of a soot nanoparticle highlighting commonly quantified properties which are relevant for
81 assessing the health and climate impact of such particles including the mobility diameter, d_m (broken line), primary
82 particle diameter, d_p (red solid line) and Organic Carbon (brown shaded area) to Total Carbon ratio, OC/TC. The
83 inset shows a high-resolution transmission electron micrograph (HRTEM) of a soot primary particle, from enclosed
84 spray combustion of jet fuel produced at an equivalence ratio of 1.25 (Trivanovic et al., 2022), where the individual
85 graphene layers can be seen. Volatile compounds that may be adsorbed on the surface usually evaporate under the
86 vacuum of the microscope so cannot be visualized easily with HRTEM.



87 The size of irregular agglomerates such as soot is quantified by equivalent diameters such as the
88 mobility diameter, d_m (Fig. 1: broken line). Using a realistic soot morphology rather than equivalent spheres in
89 climate models increases the estimated direct RF by 20% on average revealing large direct RF = 3 – 5 W/m² in
90 hot spot earth regions, in line with field observations (Kelesidis et al., 2022).

91 Furthermore, limited access to real jet engines has made it difficult to assess the efficiency of soot to act
92 as ice condensation nuclei (ICN) and thus to enhance contrail formation. To date, experiments on the ICN
93 activity of soot have been done primarily using commercial carbon blacks or miniCAST soot generated by
94 burning hydrocarbon gases (Gao et al., 2022). MiniCAST particles tend to have much larger d_m (> 100 nm) than
95 that produced by real aircraft (< 100 nm) if the organic carbon to total carbon ratio (OC/TC) is sufficiently small
96 (Durdina et al., 2016). Recently, enclosed spray combustion of jet A1 fuel has been shown to be a promising
97 laboratory surrogate for aircraft soot produced at high thrust (i.e. cruise) with sufficiently small d_m and OC/TC
98 (Trivanovic et al., 2022). This is important for the calibration of optical instruments which may be sensitive to
99 the OC/TC ratio in addition to particle morphology (Durdina et al., 2016).

100 Technology for battery-electric or hydrogen-powered planes will not be available in the short-to-
101 medium term for long-haul flights (Schäfer et al., 2019). Significant investment in airport infrastructure would
102 be needed to accommodate such changes in technology (Agnolucci et al., 2013). Emissions from aviation need to
103 be addressed urgently to meet climate goals and prevent further health degradation and mortality from air
104 pollution. However, aircraft engines have many competing demands including continued reduction of gaseous
105 emissions, CO₂ net-zero goals, safety requirements and regulations on noise. Thus, a firm understanding of the
106 environmental and health impacts of soot as well as a fundamental understanding of its formation and growth in
107 aircraft engines is essential for weighing the costs and benefits of mitigation strategies. The regulatory term
108 nvPM refers to particles that remain solid when heated to 350 °C. In aircraft emissions, this is primarily soot and
109 concentrations are measured with instruments designed for soot with a low OC/TC ratio (Lobo et al., 2015b) so
110 the terms nvPM and soot will be used interchangeably. Regulations on aircraft emissions apply only to turbofan
111 and turbojet engines with rated thrust > 26.7 kN. As such, most scientific research has been conducted on
112 engines in this category and will also be the category discussed in this paper. However, it is worth noting that
113 small business jets with thrusts < 26.7 kN may produce more nvPM emissions than large aircraft such as the
114 Boeing 737 which do fall under the ICAO regulations and need further research for accurate emissions
115 inventories (Durdina et al., 2019). In addition, while the European Union (EU) voted to ban leaded aviation
116 gasoline (Avgas) used in small piston-engine aircraft in 2022, most other countries still allow its use and it is
117 now considered one of few major sources of ambient lead in the US (National Academies of Sciences
118 Engineering and Medicine, 2021). Possible mechanisms for the formation and dynamics of soot from regulated
119 jet engines will be discussed. Then, strategies already in use or under development for the elimination of jet
120 engine soot emissions will be reviewed.

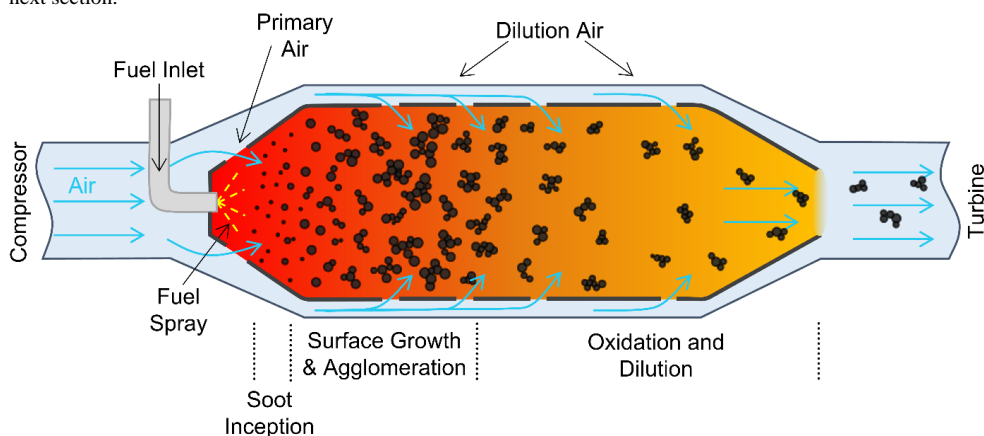
121 2. Formation and dynamics of aircraft soot

122 Although aircraft combustor design can vary significantly, the soot produced by aircrafts have some
123 morphological and compositional differences from other sources such as diesel engines. Aircrafts tend to
124 produce soot with median d_m in the range of 8 (Durdina et al., 2021) to 60 nm (Abegglen et al., 2015). Such
125 small d_m are associated with greater lung deposition efficiency (Rissler et al., 2012) and translocate from the
126 lungs to other organs more effectively than particles with d_m > 100 nm (Casseo et al., 2013). The OC/TC tends to
127 be quite low (< 25%) (Marhaba et al., 2019) when the aircraft operates at high thrust (> 50%) while the reverse
128 is true at low thrust. The OC/TC influences the optical properties of soot and thus its RF (Kelesidis et al., 2021).
129 Aircraft soot has PP diameters, d_p (Fig. 1: solid line), from approximately 5 (Liati et al., 2019) up to 24 nm with
130 lower thrusts tending to produce smaller d_p (Liati et al., 2014) which influences soot reactivity (Messerer et al.,
131 2006) and optical properties (Kelesidis et al., 2020). These same properties are also influenced by PP
132 nanostructure which is related to their maturity (Baldelli et al., 2020). Aircraft tend to produce rather disordered
133 soot with a turbostratic structure with more defects on its surface than the bulk (Parent et al., 2016). The
134 conditions under which soot forms determine its final morphology and composition and *vice versa* (Vander Wal
135 et al., 2010).

136 Figure 2 depicts the cross-section of a single annular aircraft combustor (SAC), one of the common
137 combustor designs in modern engines. The combustor is typically an annular tube that receives high pressure air
138 from the compressor, adds energy to the system through combustion and uses it to drive the turbine. Liquid jet
139 fuel is injected at one end of the SAC, typically with a swirling mechanism to atomize the fuel, promoting
140 evaporation. However, perfect mixing is not achieved. So locally fuel-rich pockets allow for soot formation even
141 if the global mixture is fuel-lean. Where the fuel is injected, there is significant recirculation allowing soot to
142 grow in these fuel-rich pockets (Gkantonas et al., 2020). When there is insufficient oxygen for complete



143 conversion to carbon dioxide, fuels decompose into radicals and intermediate species, such as acetylene which
144 then grow into small aromatics (Wang, 2011). These aromatic compounds eventually evolve into polycyclic
145 aromatic hydrocarbons (PAHs) which are the key gaseous precursors to soot (Frenklach, 2002). The presence of
146 these soot precursors has been confirmed experimentally with atomic force microscopy (Commodo et al., 2019).
147 With respect to aviation, experimental studies have shown a correlation between jet fuel aromatic content,
148 sooting tendency (Yang et al., 2007) and nvPM emissions (Brem et al., 2015). So, fuel composition plays a key
149 role in the formation of soot and thus provides one possible route for its elimination as discussed in detail in the
150 next section.



151
152 **Figure 2: A simplified schematic of an aircraft single annular combustor (SAC) adapted from Foust et al. (2012) with**
153 **a qualitative depiction of the soot dynamics from soot inception to surface growth & agglomeration and then**
154 **oxidation before being vented to the turbine and eventually the exhaust.**

155 Although the exact mechanisms of soot nucleation (i.e. the transition from the gas to solid phase) are still an
156 area of active research (Carbone et al., 2023), the dynamics of soot inception (Sharma et al., 2021) and growth
157 from nascent to mature soot (Kelesidis et al., 2017b) leading to its final structure are becoming better
158 understood. Nascent soot particles are as small as $d_m \sim 2$ nm (Camacho et al., 2015), amorphous (Commodo et
159 al., 2017) and liquid-like (Kholghy et al., 2013) with a carbon to hydrogen (C/H) ratio < 2 (Schulz et al., 2019).
160 As they age, nascent soot carbonizes (lose hydrogen) and solidifies (Dobbins, 2002). Soot then simultaneously
161 undergoes surface growth and agglomeration (Kelesidis et al., 2017a). Surface growth of soot is well described
162 by the hydrogen-abstraction carbon-addition (HACA) mechanism (Frenklach, 2002) although other pathways
163 have also been proposed (Wang, 2011). During the first few milliseconds of particle growth, surface growth
164 precursors are depleted then agglomeration takes over as the primary growth mechanism and d_m increases
165 markedly while d_p stays approximately constant (Kelesidis et al., 2017a). In the free molecular regime, particles
166 grow into large agglomerates through ballistic cluster-cluster coagulation while in the continuum regime this
167 becomes diffusion-limited cluster agglomeration. Particles which coagulate in the free molecular regime have a
168 slightly more compact structure than those in the continuum regime as shown by their asymptotic mass fractal
169 dimensions of 1.91 and 1.78, respectively (Goudeh et al., 2015).

170 This soot growth sequence has been observed and quantified for soot formation in premixed flames, diesel
171 engines, miniCAST soot generator (Kelesidis et al., 2017b) and even for enclosed spray combustion of Jet A1
172 fuel resulting in aircraft-like soot (Trivanovic et al., 2023). After primary air injection for the initial combustion,
173 dilution air is added at various locations along the combustor length. This oxidizes a sizable portion of the soot
174 which was initially created. Transmission Electron Microscopy (TEM) has shown that aircraft soot is
175 significantly oxidized and the small d_m may be in part due to fragmentation of larger agglomerates after
176 extensive oxidation (Vander Wal et al., 2014). So, in the early stages of the combustor the number and size of
177 soot is likely larger than what is eventually emitted. The final morphology of the particles, including the d_p , d_m
178 and number of PPs per agglomerate, n_p , depends on the initial volume fraction, residence time, temperature and
179 pressure (Kelesidis et al. 2023).

180 While conditions can vary significantly depending on the engine, soot in an aircraft combustor
181 experiences both high temperature and pressure. In addition, pressures are increased at high thrust which has
182 been correlated with increased soot concentration and size (Chu et al., 2023). Higher pressures improve the
183 efficiency of engines and so as engine materials have been improved to withstand higher pressures, the pressure
184 ratios in engines have also increased. So, soot may begin growing in the free molecular regime but enters the



185 transition regime as it grows, in particular at high thrust, when pressures are the highest and soot particles tend to
186 grow to the largest sizes. This is in line with mass-mobility measurements of aircraft soot which shows an
187 increase in the mass-mobility exponent, D_{fm} , from 1.86 ± 0.37 to 2.79 ± 0.07 as thrust increases from 7 to 118%,
188 respectively (Abegglen et al., 2015). However, mass-mobility measurements are not part of the regulatory
189 framework for aircraft nvPM.

190 Low thrusts lead to the longest soot residence time in the combustor but tend to produce the smallest
191 particles both in terms of d_m and d_p which can be attributed to the smaller amount of fuel resulting in a lower
192 volume fraction of nascent soot (i.e. less nucleation) and allowing for a longer residence time in oxygen rich
193 zones which oxidizes the soot reducing both the number and size of particles (Durdina et al., 2014). At the same
194 time, the OC/TC increases at low thrust which could be attributed to the poor combustion efficiency at these
195 conditions. At high thrust the residence time is short but initial number concentrations are higher due to high fuel
196 flow. The time in oxidating zones is reduced also, resulting in a larger number concentration, d_p (Liati et al.,
197 2014) and d_m (Abegglen et al., 2015). Simulations of aircraft combustors have shown that soot forms
198 intermittently in locally rich regions of the flame and, due to recirculation, soot spends 4 – 5 times longer in the
199 combustor than the fluid time scales (Chong et al., 2018b). The high-temperature residence time of soot in a
200 combustor can only be estimated from simulations that account for the geometry, fluid flow rates, temperature
201 and pressure in a given combustor.

202 Modeling soot emissions accurately remains a challenge (Chong et al., 2018a) because soot formation in
203 combustors is intermittent. So, simulations must take place over a large time frame to achieve a statistically
204 representative time-averaged result (Franzelli et al., 2023). Furthermore, the transport and chemistry of soot must
205 be solved simultaneously in order to capture the real volume fraction, f_v , and particle size distributions (PSD)
206 (Gkantonas et al., 2020). The most detailed simulations to date have utilized laboratory combustors such as the
207 Cambridge Rich Quench Lean (RQL) burner (Gkantonas et al. 2020, Fig. 2). These laboratory burners are
208 optically accessible for laser diagnostics allowing for a detailed comparison to the evolution of soot f_v and PSD.
209 However, the laboratory burners use ethylene, a gas, instead of liquid jet fuel and pressures are up to 5 bar
210 (Chong et al., 2018a). Modern aircraft engines may have pressures up to an order of magnitude higher than this
211 at certain conditions (Nguyen et al., 2019). Nonetheless, such simulations can give insight into the formation and
212 growth of soot in aircraft combustors capturing some of the trends observed experimentally. Specifically,
213 simulations show that soot forms near the shear layers between the fuel and oxidizer streams and then enters an
214 inner recirculation zone where it grows further (Gkantonas et al., 2020). Fuel rich pockets can also break off
215 from the main jet and become entrained in the recirculation zone driving the intermittent soot growth within the
216 combustor (Chong et al., 2018a). Soot was shown to grow by both acetylene-based surface growth (e.g., HACA)
217 and condensation via aromatics (Gkantonas et al., 2020). Simultaneously, significant oxidation reduces the
218 particle size and can induce fragmentation increasing the number concentration (Gkantonas et al., 2020) which is
219 supported by experimental data (Vander Wal et al., 2014). Introduction of dilution air part way through the
220 burner oxidizes soot in the lean combustion zone as well as lowers the rate of soot formation near the nozzle
221 (Chong et al., 2018a). Higher pressures in the model combustor result in larger soot f_v , a trend which was
222 captured by simulations but the total f_v for the high pressure condition was underpredicted by a factor of 4
223 (Chong et al., 2018a). Therefore, simulations can give insight into the formation of soot in aircraft combustors
224 but significant improvements are needed to have truly predictive models which can aid in combustor design
225 (Franzelli et al., 2023). It is worth noting that these simulations focus on capturing the number and mass
226 emissions from combustors, but do not seem to account for the realistic morphology of soot particles which are
227 highly irregular agglomerates rather than spheres. The assumption that soot is spherical rather than an
228 agglomerate with polydisperse primary particles can significantly change the resulting estimate of soot d_m ,
229 number and, most importantly, f_v (Kelesidis and Goudeli, 2021).

230 3. Means for the elimination of aircraft soot

231 3.1 Sustainable aviation fuels

232 Alternative fuels are attractive due to their unique position as a drop-in solution for reducing CO₂ emissions as
233 these fuels can be used directly in existing engines. The ICAO specifies fuels must be “completely
234 interchangeable and compatible with conventional jet fuel” in order to prevent the safety risks of mishandling
235 and high costs of additional infrastructure (ICAO, 2018). Sustainable Aviation Fuels (SAF) are produced from
236 biological feedstocks (e.g. soybeans, sugarcane, biomass, etc.) (Staples et al., 2018). These are converted into
237 liquid hydrocarbon fuels through processes such as Hydroprocessed Esters and Fatty Acids (HEFA), Fischer-
238 Tropsh (F-T) or Alcohol-to-Jet (ATJ) to name a few (Brooks et al., 2016). Lower Carbon Aviation Fuels
239 (LCAF) or e-fuels use CO₂ capture and sustainable energy sources such as solar to produce synthetic jet fuels



240 (Schäppi et al., 2022). The CO₂ reduction from such fuels comes primarily from the synthetic or biological CO₂
241 captured during the production process. Actual CO₂ released from the engine remains about the same as
242 conventional jet fuel. So, a Life Cycle Analysis (LCA) is needed to account for the so-called Well-to-Wake
243 emissions (Han et al., 2013). The total reduction in Green House Gas (GHG) emissions will depend on both the
244 GHG emissions associated with production of the petroleum based jet fuel as well as the net GHG emissions
245 from growing, transporting and burning the SAF fuels. The ICAO certifies alternative fuels as SAF or LCAF
246 based on a standardized LCA. While the exact reduction in GHGs will change as technologies evolve, an LCA
247 of the best case scenarios show up to a 68% reduction in CO₂ emissions if SAFs account for > 85% of all
248 aviation fuels (Staples et al., 2018).

249 In addition to reducing net-CO₂ emissions, SAFs and LCAFs also have the potential to reduce soot
250 emissions and thus the health impact and non-CO₂ radiative forcing of aircraft emissions which is typically
251 excluded from LCA analysis (Staples et al., 2018). These fuels tend to have a lower aromatic content than fossil
252 fuels which has been correlated to the number of particles emitted by an aircraft (Brem et al., 2015). As
253 discussed previously, aromatic species are key precursors to soot formation and thus a decrease in fuel aromatics
254 may reduce the rate of soot nucleation. The hydrogen-to-carbon ratio (H/C) of the fuel has been shown to have
255 an even greater anti-correlation with aircraft soot emissions than fuel aromatic content (Brem et al., 2015). While
256 H/C has long been associated with the sooting tendency of a fuel (Yang et al., 2007), the mechanism for this is
257 less clear as it is difficult to separate from effects such as lower flame temperatures (Xue et al., 2019). Blends
258 of a HEFA-based SAF with Jet A1 up to 50% (the current upper limit for a SAF blend) showed a ~35% reduction
259 in number based nvPM and ~60% reduction in mass based nvPM (Lobo et al., 2015a). These reductions
260 correlated best with the H/C content of the blends. The size distributions of the soot produced shifted to smaller
261 mobility diameters from $d_m = 49$ to 22.5 nm and narrowed the distribution from a geometric standard deviation,
262 $\sigma_g = 1.99$ to 1.58 with pure Jet A1 and a 50% blend, respectively (Lobo et al., 2015a). With pure Jet A1, the σ_g
263 approaches that of the self-preserving limit for agglomerates coagulating in the free-molecular regime (Goudeh
264 et al., 2015) while the σ_g produced with the SAF blends are significantly smaller. This could be due to the
265 decreased number concentration from extended surface growth and less agglomeration. Currently, alternative
266 fuels are designed primarily with the goals of reducing life-cycle CO₂ emissions and matching the properties of
267 conventional jet fuels. However, there is an opportunity to also optimize jet fuel composition for minimum soot
268 emissions. Schripp et al. (2021) showed that different SAF could be blended to obtain a desired H/C, while
269 maintaining regulatory specifications for jet fuels. Soot emissions of these fuels were first tested in a laboratory
270 flame, then the optimal mixture was used in a real jet engine to confirm the trends seen in the laboratory
271 resulting in emission reductions of particle mass and number by 29 and 37%, respectively, when using a 38%
272 SAF blend with Jet A1 (Schripp et al., 2021). Laboratory tests are essential for speeding up the design of
273 alternative fuels since real jet engines are inaccessible to many researchers and too costly to operate for initial
274 screening tests. A standardized flame for assessing the sooting properties of jet fuels would assist in the
275 development of alternative fuels however, there is currently no standardized method for such experiments.
276 Enclosed spray combustion is a promising unit for such in lab approaches (Trivanovic et al., 2022).

277 Several publications have shown that the benefits of a SAF blend are thrust-dependent. For example, a
278 32% blend of HEFA-synthetic paraffinic kerosene and Jet A1 at idle operation showed a 60 and 70% reduction
279 in number- and mass-based nvPM, respectively (Durdina et al., 2021). The same blend at 65% thrust resulted in
280 only a 12% reduction in number-based nvPM and at take-off the reduction was only 7%. In this case, the use of
281 such SAF blends may improve local air quality by reducing emissions in the vicinity of airports but may not
282 make a significant impact on cruise conditions which are most concerning for climate change. It is worth noting
283 that the majority of studies on aircraft soot emissions are done at ground level which has significantly different
284 atmospheric conditions than cruise in the upper atmosphere. Ideally, cruise emissions should be measured behind
285 an aircraft in-flight, but this is rarely done due to the cost and logistical challenges. One of the few in-flight
286 studies comparing conventional jet fuel to a 50% HEFA blend showed a 50 and 70% reduction in particle
287 number and mass emissions, respectively, behind an aircraft with a medium thrust setting of ~ 50% (Moore et
288 al., 2017). At the high thrust setting, the particle number reduction was only 25% (Moore et al., 2017),
289 supporting the trend observed on the ground. The wide range of values listed here highlights the need for more
290 studies both at the ground level and in-flight.

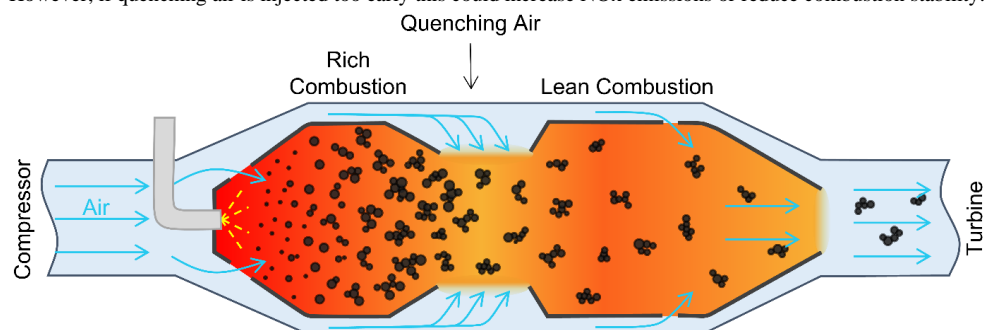
291 Currently, SAF must be blended with conventional jet fuel (up to 50%) for safety reasons although
292 100% blends may be allowed by 2030. In practice, supply issues keep the use of SAF low accounting for an
293 estimated 0.1 – 0.15% of global jet fuel use in 2022 despite a tripling in the supply of SAF from 2021 to 2022. If
294 the SAF supply is limited and individual flights only have a very small fraction of SAF in the fuel, there will
295 likely be no effect on the soot emissions (Lobo et al., 2015a). So, while alternative fuels could provide a short-
296 term solution to reducing aircraft emissions, the speed at which this is adopted is still limited. Targeted use of the



297 limited SAF supply could be used in the short term to maximize the benefits of such fuels while supply is
298 limited. For example, contrails with the greatest warming effect are commonly at dusk during the winter (Teoh et
299 al., 2022a) so fueling flights at such times with high SAF blends could have the biggest benefit. One analysis
300 found that compared to a 1% SAF blend for all transatlantic flights, fueling the 2% of flights producing the
301 highest RF with a 50% SAF blend could take the total RF reduction from 0.6% up to 6% (Teoh et al., 2022b).
302 The European Commission and the US have implemented policies to mandate the uptake of SAF which may
303 prohibit the targeted use of SAF. For example, starting in 2025 it will be required that “all aviation fuel supplied
304 to aircraft operators at (European) Union airports contains a minimum share of SAF” (European Commission,
305 2021). Thus, while the supply of SAF is limited, it will be used in more aircraft at lower blending ratios missing
306 an opportunity to reduce soot emissions. Intelligent changes to policy on the use of alternative fuels could thus
307 reduce the net-RF of aviation without needing to increase the supply of SAF and LCAF.

308 3.2 Aircraft Combustor Design & Operation

309 The limitations of alternative jet fuels highlight the continued need for improved and novel engine technologies
310 which could be used also with alternative fuels to minimize the total impact of aviation on the environment.
311 Here, only combustion engines will be considered as electric aircrafts are estimated to account for only a quarter
312 of all passenger-miles in 2050 (Prabhakar et al., 2022). Since nvPM regulations only recently came into effect,
313 most aircraft combustors are designed primarily to lower NO_x, but some designs can also reduce soot.
314 Alternative fuels have not been shown to reduce NO_x emissions compared to conventional jet fuel (Moore et al.,
315 2017). Combustor designs must balance limits for all regulated gas and particulate emissions, fuel efficiency,
316 safety and cost. Rich Quench Lean (RQL) combustors have been used by the aviation industry since at least the
317 1980s to reduce NO_x emissions while maintaining sufficient combustion stability (Novic et al., 1983). Today,
318 they are the most common type of combustor listed in the ICAO emissions database (ICAO Aircraft Engine
319 Emissions Databank, 2023). Briefly, RQL combustors have three zones, depicted in Figure 3. First, there is a
320 fuel-rich zone that allows for more stable combustion which is important for the safety of the aircraft. Rich
321 conditions have lower combustion efficiency and promote the formation of soot, UHCs, and CO. In the
322 quenching zone, a large volume of cool air is injected to provide oxygen for completing the conversion of UHCs
323 and CO to CO₂ while lowering the temperature to minimize NO_x formation. The air flow for the rich combustion
324 stage and quenching zone are controlled separately and further dilution air may be added before the gases are
325 sent to the turbine. Although the mixing and residence times in RQL combustors were originally optimized for
326 reducing NO_x (Rizk and Mongia, 1990) proper design and operation can also reduce soot emissions through
327 oxidation during the lean burn stage. In fact, it was shown that a judicious injection of fresh oxygen in a manner
328 similar to RQL combustors can promote oxidation of soot removing up to 99.6% of the initial soot volume
329 fraction from jet fuel combustion (Kelesidis et al., 2023b). When quenching air is introduced farther downstream
330 in the combustor, soot has more time to form and grow. Hence, oxidation is less effective. Earlier injection of air
331 with sufficient turbulent mixing has the opposite effect, minimizing soot emissions (El Helou et al., 2021).
332 However, if quenching air is injected too early this could increase NO_x emissions or reduce combustion stability.

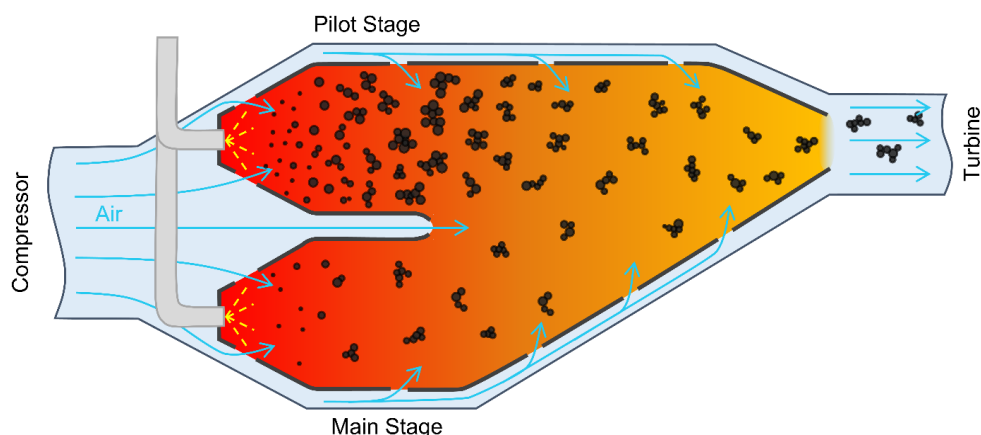


333
334 **Figure 3: A simplified schematic of a Rich Lean Quench (RQL) aircraft combustor adapted from Rizk and Mongia**
335 **(1990) where there is first a fuel rich combustion zone, followed by a large flow of quenching air to lower the**
336 **temperature and dilute to a globally lean combustion zone. The dynamics of soot are qualitatively depicted from**
337 **inception to surface growth, agglomeration and oxidation.**

338 In 1995, the first Double Annular Combustor (DAC) was used commercially. This combustor design
339 has two stages as the name implies, depicted in Figure 4. At low thrust (e.g., idle) only the pilot stage is used
340 with a low air to fuel ratio and low flowrate to ensure good ignition and to reduce CO and UHC emissions.

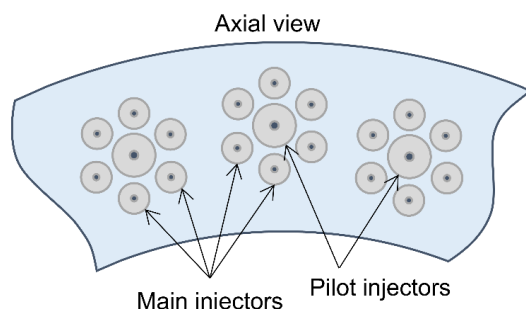


341 When sufficiently high thrust is achieved, both the pilot and main stage are ignited with a high air to fuel ratio
342 (lean burn) and high flowrates (Boies et al., 2015). This had the desired effect of reducing the NO_x emissions
343 over the LTO cycle by ~30% compared to a single annular combustor on the same engine (Mongia, 2007). Soot
344 emissions from a DAC equipped engine vary significantly with thrust. At low thrust, when only the pilot stage is
345 ignited, soot emissions are high, and increase with increasing thrust in both number and mobility diameter (Boies
346 et al., 2015). When both stages are ignited at thrust ~25%, the soot concentration and size drops significantly
347 (Boies et al., 2015). Similarly, a DAC using only the pilot stage showed an increased mass concentration of
348 organic particulate matter compared to when both stages were used (Lobo et al., 2015b). The morphology of soot
349 produced in both stages is in the range observed in other combustors.



350
351 **Figure 4: Simplified schematic of a Double Annular Combustor (DAC) adapted from Foust et al. (2012) and a**
352 **qualitative depiction of the dynamics of soot surface growth, agglomeration and oxidation within the combustor.**

353 As demonstrated by the low emissions of DAC when operated in the lean combustion mode, lean burn
354 engines have the potential for extremely low emissions if the combustion stability issues can be overcome. In
355 fact, lean combustion technologies typically produce an order of magnitude less soot than an RQL combustor
356 (Liu et al., 2017). Lean burn combustors were first developed for stationary gas turbines used for energy
357 generation where safety requirements are less strict and are now being transferred to aviation as technology
358 improves. Such technologies include Lean Direct Injection (LDI) or the Multipoint Lean Direct Injection concept
359 (MLDI) (Liu et al., 2017). Direct injection is used to reduce the risk of autoignition that comes with premixed
360 combustion. The use of multiple injectors, depicted in Figure 5, along with intense mixing creates conditions
361 similar to lean, premixed combustion. In an LDI combustor a central pilot injector is surrounded by multiple
362 main fuel injectors with little to no dilution added after the initial air supply near the fuel injectors. The MLDI
363 concept is similar to the LDI combustor with an altered injector layout. Globally lean combustion with good
364 mixing is unfavorable for soot production as there are few locally fuel-rich areas. At the same time, low
365 temperatures from the lean burn reduce NO_x emissions significantly (Liu et al., 2017). Regulatory measurements



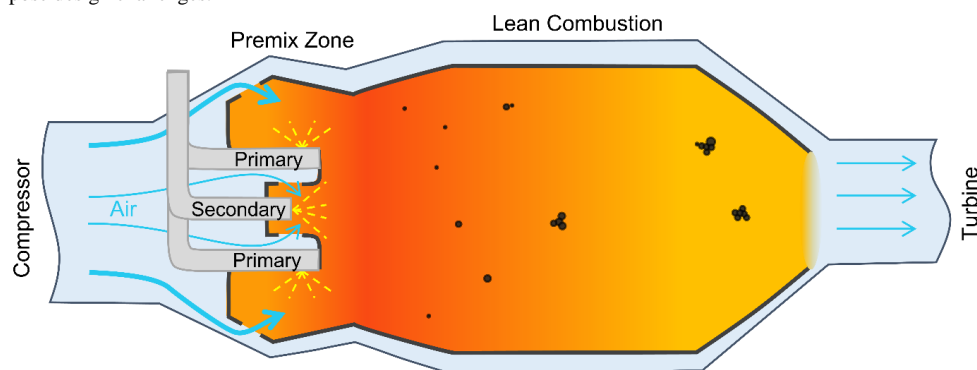
366
367 **Figure 5: A simplified schematic of a Lean Direct Injection (LDI) combustor adapted from Fric (1995) which features**
368 **a central pilot injector surrounded by multiple main injectors. These combustors usually have most or all the air flow**
369 **into the combustor around the fuel injectors without subsequent dilution to provide intense mixing for lean**
370 **combustion with close to premixed combustion.**



371 of nvPM emissions from an LDI combustor show nvPM mass and number emission levels on par with RQL
372 combustors with similar rated thrusts (ICAO Aircraft Engine Emissions Databank, 2023). To the best of our
373 knowledge, no studies have characterized the size, morphology or chemical composition of soot from an LDI
374 equipped engine. The limited data for such combustors makes the real emissions performance of such an engine
375 difficult to assess.

376 Lean Premixed Prevaporized (LPP) combustors aim to completely vaporize the jet fuel prior to ignition
377 in order to have lean, premixed combustion (Figure 6). Without locally fuel-rich conditions, little to no soot will
378 form. As with the LDI combustors, there is little dilution after the initial injection of primary air for combustion.
379 Premixed combustion with high pressures comes with a risk of autoignition in the mixing zone so careful design
380 of the combustor is needed to prevent such instabilities. These combustors use special fuel injectors to achieve
381 near-premixed lean combustion conditions which tend to form significantly less soot. Both the LDI and LPP
382 combustor designs achieve stable combustion through complex combustor design which could lead to increased
383 cost and maintenance. So, lean conditions are favorable for emissions reduction but come with engineering
384 challenges. Theoretically, new jet fuels with lower lean blow-off (LBO) limits could extend the lean operating
385 range of an engine and conversely, fuels with an insufficient LBO could pose a safety risk (Undavalli et al.,
386 2023).

387 Recently, a novel research engine called the Lean Azimuthal Flame (LEAF) combustor (not yet in
388 commercial use) using “flameless oxidation” has been developed for soot-free and low NO_x combustion
389 (Oliveira et al., 2021). This concept can be further improved through co-combustion of small amounts of
390 hydrogen which extends the operating window (Miniero et al., 2023). The use of hydrogen helps to stabilize the
391 combustion without the use of a fuel-rich pilot flame that can increase soot production as with the DAC
392 combustors. Such concepts which require an additional fuel that cannot be used in all engines require
393 significantly more capital to implement because additional infrastructure needs to be built to support, for
394 example, hydrogen storage and fueling. Furthermore, such parallel infrastructure poses a safety risk if an aircraft
395 is filled with the wrong fuel and therefore such solutions are not promoted by the ICAO (2018). So, combustors
396 which achieve lean, premixed conditions are promising for achieving both low soot and low NO_x emissions but
397 pose design challenges.

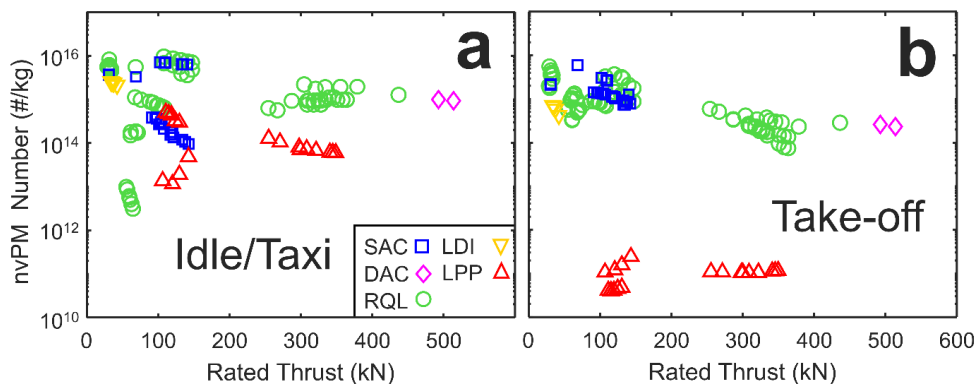


398 **Figure 6: A simplified schematic of a Lean Premixed Prevaporized (LPP) combustor adapted from Foust et al. (2012)**
399 **which contains multiple injectors that spray fuel into the premix zone where the jet fuel completely vaporizes without**
400 **ignition. Then, in the combustion zone the premixed fuel is ignited under fuel-lean conditions which nearly eliminate**
401 **soot while low temperatures prevent the formation of NO_x.**
402

403 The ICAO provides a public database of regulated emissions with the earliest nvPM emission test dates
404 starting in 2014 (ICAO Aircraft Engine Emissions Databank, 2023). These data are collected and reported by the
405 engine manufacturers following the standards laid out in the ICAO Annex 16 for engine emissions certification
406 (ICAO, 2017). Emissions are tested across the entire LTO cycle which includes idle/taxi (7% thrust), approach
407 (30%), climb-out (80%) and take-off (100%) for both nvPM mass and number. Figure 7 shows the nvPM
408 number emissions normalized by the fuel flow (#/kg) at (a) idle/taxi and (b) take-off for simplicity, although
409 approach and climb-out data are also available (ICAO Aircraft Engine Emissions Databank, 2023). Mass nvPM
410 data shows similar trends. Values for approach and climb-out tend to fall between those measured at the
411 extremes for both number and mass nvPM. Combustor names are provided for all entries in the database and can
412 be grouped by type if sufficient information is given by the manufacturer. The RQL combustors make up the
413 majority of reported data (134 entries), followed by SAC (38), LPP (27), LDI (7) and DAC (2). The SAC
414 (squares) have some of the highest emissions in the database, but a group of SAC are approximately an order of



415 magnitude lower at idle/taxi (Fig. 7a). These lower emission SAC are modified for better performance (CFM
416 Tech Insertion) which seems to improve emissions at low (7 and 30%) thrust with little change at high (80 and
417 100%) thrust. The data for RQL combustors (circles) have the most variation quite likely due to the fact that
418 there are significantly more entries for RQL combustors compared to all other combustor types. This highlights
419 the fact that RQL burners can have quite low particulate emissions if designed and operated properly,
420 particularly for engines with lower static rated thrust. At take-off (Fig. 7b), the LPP combustors (triangles)
421 clearly outperform all other combustors in the database. At idle/taxi (Fig. 7a) LPP combustors still perform well
422 but some RQL and modified-SAC combustors have similar or lower emissions. In an LPP combustor, all
423 injectors are on during high thrust operation and premixed combustion can be achieved resulting in lower
424 emissions. Conversely, at low thrust only some of the injectors are used to lower the power output without
425 creating conditions which are too lean for stable combustion which may explain the higher emissions at idle/taxi
426 compared to take-off. A similar phenomenon has been observed in scientific studies of DAC engines where
427 emissions were reduced significantly when both combustor stages were in use at approximately thrusts > 30%
428 (Boies et al., 2015). The small number of entries for DAC and LDI combustors makes it difficult to draw
429 conclusions about such combustors but the data that are provided for both fall in approximately the middle of the
430 nvPM emission range. So, at present LPP combustors seem to perform at least as well as other combustors at
431 idle/taxi and significantly reduce emissions at take-off resulting in the lowest overall emissions in the ICAO
432 database. It is worth noting that engine operation can also reduce emissions, for example reduced thrust take-off
433 has been shown to reduce fuel consumption, NO_x and black carbon (soot) emissions by 1.0–23.2%, 10.7–47.7%,
434 and 49.0–71.7% respectively (Koudis et al., 2017).



435
436 **Figure 7: The nvPM number as a function of an engine's rated thrust at (a) idle/taxi (7% thrust), (b) take-off (100%).**
437 **Combustor types represented in the database include SAC (squares), DAC (diamonds), RQL (circles), LDI (inverted**
438 **triangles), LPP (triangles). The total nvPM number is normalized by the fuel flow (kg).**

439 While the ICAO database provides information on the mass and number of nvPM emissions, it does not
440 include any morphological or chemical characterization of the particles. Furthermore, the data are collected by
441 the engine manufacturers, rather than independent researchers. Thus far, the vast majority of academic studies on
442 soot emissions from aircraft engines have been conducted on large commercial aircraft (rated thrust >26.7 kN)
443 most with SAC combustors (Liati et al., 2014; Beyersdorf et al., 2014; Marhaba et al., 2019; Parent et al., 2016;
444 Abegglen et al., 2015; Johnson et al., 2015; Elser et al., 2019). A few studies have explored soot from DAC
445 (Lobo et al., 2015b; Boies et al., 2015; Johnson et al., 2015) and RQL (Saffaripour et al., 2017; Delhaye et al.,
446 2017; Brem et al., 2015) engines. The limited number of studies characterizing soot emissions from 'low
447 emission' engine technology highlights the need for more research on such engines if they will be adopted in the
448 future. Commercial deployment of new engine technologies takes a significant amount of time and money and
449 so, when a new technology is deployed it remains in use for many years with the life span of an average aircraft
450 spanning from 20 – 30 years (Ceruti et al., 2019). This makes it essential to identify which technologies offer the
451 best emissions profile before it is commercially scaled up, for example through the use of computational fluid
452 dynamics (CFD).



453 4. Conclusions

454 Soot from aviation has a negative effect on human health and can contribute to climate change through direct
455 radiative forcing and increasing the formation of persistent contrails. New regulations have been put into place to
456 limit soot emissions in addition to other pollutants such as NO_x, UHC and CO. The strategies for reducing one
457 type of pollutant may increase another with soot and NO_x emissions often at odds with one another. Non-CO₂
458 aircraft emissions are estimated to be two thirds of aviation's net-RF, but the uncertainties associated with the
459 non-CO₂ terms are very high. The difficulty in reducing soot emissions from aviation comes primarily from the
460 competing requirements which include safety, reduction of gaseous pollutants and cost. A better understanding
461 of the role of soot and other non-CO₂ emissions is needed to properly assess trade-offs between design
462 requirements and avoid improving emissions of one pollutant while increasing another's or compromising
463 safety.

464 Aircrafts tend to produce soot with relatively small d_m which has greater health impacts than larger soot
465 particles. Soot nucleates in locally fuel-rich zones (created by the jet fuel spray) then grows through surface
466 growth, condensation and agglomeration. The OC/TC ratio of aircraft soot depends on thrust. Low thrust is
467 associated with high OC/TC and high with low OC/TC. Extensive oxidation reduces the number concentration
468 and size of soot resulting in smaller particles than other combustion sources (e.g. diesel). Significant progress is
469 still needed to accurately quantify this process in realistic aircraft combustors. Some progress has been made in
470 recent years matching experimental data from laboratory combustors but there are important differences between
471 laboratory combustors and real aircraft combustors and simulations are not yet able to match the output of these
472 simplified combustors at all conditions. The high cost and 20 – 30 year lifespan of aircraft necessitates robust
473 models to aid in combustor design and operation for further technological advancements.

474 Alternative fuels have the potential to significantly reduce soot emissions due to the lower aromatic and
475 H/C content typically associated with these fuels in addition to reductions in lifetime CO₂ emissions. Alternative
476 jet fuels can be created through processing of biological feedstocks (e.g., soybeans), typically referred to as
477 Sustainable Aviation Fuels (SAF), or through conversion of energy (e.g., solar electricity) into a liquid fuel,
478 typically referred to as Low Carbon Aviation Fuels (LCAF). Although most literature on the use of such fuels
479 does show that it reduces soot emissions, the reduction appears to be thrust dependent. So, it has the greatest
480 effect on reducing low-thrust emissions which are important for local air quality (e.g., idle) although modest
481 reductions have also been observed at high altitude cruising conditions. Several SAFs are approved for
482 commercial use but lack of sufficient supply makes it a tiny proportion of the global jet fuel supply (0.1-0.15%
483 in 2022). If SAFs are blended at small proportions with conventional jet fuel, the soot reduction benefits might
484 be hardly seen. Targeted use of high SAF blends on certain flights rather than low SAF blends for all flights
485 could be the best use of a limited resource. Supply issues likely will not be overcome soon, so policies
486 mandating the use of SAF and LCAF fuels should be designed in a way that encourages the use of a targeted
487 approach that will also lower soot emissions, not just life cycle CO₂.

488 Soot is primarily produced during fuel-rich combustion. So, throughout the years efforts have been made
489 to move toward fuel-lean combustion processes. The RQL combustors use a lean quenching stage after an initial
490 rich burn to ensure good combustion stability while still reducing NO_x and in some cases soot. The design of the
491 quenching stage is essential for balancing combustion efficiency, NO_x, and soot emissions from such engines.
492 The DAC combustors similarly take advantage of a pilot stage with low air to fuel ratios for combustion stability
493 at low thrust and a second main stage combustor which can be used at medium to high thrust for lean
494 combustion with a high air to fuel ratio. When both stages are in use, DAC combustors have very low soot
495 emissions but when only the pilot stage is used, soot emissions can be higher than in a traditional burner
496 particularly at medium-low thrust (e.g., ~20%). More recently, advances have been made on truly lean engine
497 technologies. This can be achieved either by using multiple injectors and high mixing rates to achieve nearly
498 premixed combustion or through mixing zones which allow for full evaporation of fuel before ignition. These
499 lean burn engines promise the lowest emissions of soot and NO_x due to the lower temperatures and lack of fuel-
500 rich zones. High complexity in such burners may result in higher maintenance costs. Finally, hydrogen can be
501 used to help stabilize lean combustion such as in the LEAF combustor which is both soot-free and low NO_x but
502 is still under development in academic laboratories. However, the ICAO is discouraging such solutions which
503 require fuels that are not "drop-in" (e.g. hydrogen), as incompatibilities between engines and fuels could pose
504 safety risks and require significant capital investment in infrastructure.

505 The combined use of fuels with low sooting propensity and operating at lean combustion conditions have
506 the potential to reduce or even eliminate soot emissions from aircraft engines. However, caution should be used
507 whenever there is a trade-off with other emissions (i.e. NO_x) as there is still significant uncertainty in the
508 contribution of soot to direct RF and its role in contrail formation. The development of computational models



509 which can accurately predict soot production from various combustor designs and modes of operation will be
510 essential for minimizing soot emissions from aircraft while balancing other considerations. This will rely on
511 further fundamental research to better understand soot nucleation rates to close the soot mass balance and match
512 field data.

513 **Competing interests**

514 The contact author has declared that none of the authors has any competing interests.

515 **Acknowledgements**

516 We gratefully acknowledge Christian Kubsch for proofreading this article. This research was funded by the
517 Particle Technology Laboratory, ETH Zurich, and in part by Swiss National Science Foundation
518 (200020_182668, 250320_163243 and 206021_170729) and the Natural Sciences and Engineering Research
519 Council of Canada (NSERC CGSD3-547016-2020).

520 **References**

- 521 Abegglen, M., Durdina, L., Brem, B. T., Wang, J., and Rindlisbacher, T.: Effective density and mass – mobility
522 exponents of particulate matter in aircraft turbine exhaust : Dependence on engine thrust and particle size, *J.*
523 *Aerosol Sci.*, 88, 135–147, <https://doi.org/10.1016/j.jaerosci.2015.06.003>, 2015.
- 524 Agarwal, A., Speth, R. L., Fritz, T. M., Jacob, S. D., Rindlisbacher, T., Iovinelli, R., Owen, B., Miake-Lye, R.
525 C., Sabnis, J. S., and Barrett, S. R. H.: SCOPE11 Method for Estimating Aircraft Black Carbon Mass and
526 Particle Number Emissions, *Environ. Sci. Technol.*, 53, 1364–1373, <https://doi.org/10.1021/acs.est.8b04060>,
527 2019.
- 528 Agnolucci, P., Akgul, O., McDowall, W., and Papageorgiou, L. G.: The importance of economies of scale,
529 transport costs and demand patterns in optimising hydrogen fuelling infrastructure: An exploration with
530 SHIPMod (Spatial hydrogen infrastructure planning model), *Int. J. Hydrogen Energy*, 38, 11189–11201,
531 <https://doi.org/10.1016/j.ijhydene.2013.06.071>, 2013.
- 532 Baldelli, A., Trivanovic, U., Sipkens, T. A., and Rogak, S. N.: On determining soot maturity: A review of the
533 role of microscopy- and spectroscopy-based techniques, *Chemosphere*, 252, 126532,
534 <https://doi.org/10.1016/j.chemosphere.2020.126532>, 2020.
- 535 Beyersdorf, A. J., Timko, M. T., Ziemba, L. D., Bulzan, D., Corporan, E., Herndon, S. C., Howard, R., Miake-
536 Lye, R., Thornhill, K. L., Winstead, E., Wey, C., Yu, Z., and Anderson, B. E.: Reductions in aircraft particulate
537 emissions due to the use of Fischer-Tropsch fuels, *Atmos. Chem. Phys.*, 14, 11–23, <https://doi.org/10.5194/acp-14-11-2014>, 2014.
- 539 Bock, L. and Burkhardt, U.: The temporal evolution of a long-lived contrail cirrus cluster: Simulations with a
540 global climate model, *J. Geophys. Res.*, 121, 3548–3565, <https://doi.org/10.1002/2015JD024475>, 2016.
- 541 Boies, A. M., Stettler, M. E. J., Swanson, J. J., Johnson, T. J., Olfert, J. S., Johnson, M., Eggersdorfer, M. L.,
542 Rindlisbacher, T., Wang, J., Thomson, K., Smallwood, G., Sevcenco, Y., Walters, D., Williams, P. I., Corbin, J.,
543 Mensah, A. A., Symonds, J., Dastanpour, R., and Rogak, S. N.: Particle emission characteristics of a gas turbine
544 with a double annular combustor, *Aerosol Sci. Technol.*, 49, 842–855,
545 <https://doi.org/10.1080/02786826.2015.1078452>, 2015.
- 546 Bond, T. C., Doherty, S. J., Fahey, D. W., Forster, P. M., Berntsen, T., DeAngelo, B. J., Flanner, M. G., Ghan,
547 S., Kärcher, B., Koch, D., Kinne, S., Kondo, Y., Quinn, P. K., Sarofim, M. C., Schultz, M. G., Schulz, M.,
548 Venkataraman, C., Zhang, H., Zhang, S., Bellouin, N., Guttikunda, S. K., Hopke, P. K., Jacobson, M. Z., Kaiser,
549 J. W., Klimont, Z., Lohmann, U., Schwarz, J. P., Shindell, D., Storelvmo, T., Warren, S. G., and Zender, C. S.:
550 Bounding the role of black carbon in the climate system: A scientific assessment, *J. Geophys. Res. Atmos.*, 118,
551 5380–5552, <https://doi.org/10.1002/jgrd.50171>, 2013.
- 552 Brem, B. T., Durdina, L., Siegerist, F., Beyerle, P., Bruderer, K., Rindlisbacher, T., Rocci-Denis, S., Andac, M.
553 G., Zelina, J., Penanhoat, O., and Wang, J.: Effects of Fuel Aromatic Content on Nonvolatile Particulate
554 Emissions of an In-Production Aircraft Gas Turbine, *Environ. Sci. Technol.*, 49, 13149–13157,
555 <https://doi.org/10.1021/acs.est.5b04167>, 2015.
- 556 Brooks, K. P., Snowden-Swan, L. J., Jones, S. B., Butcher, M. G., Lee, G. S. J., Anderson, D. M., Frye, J. G.,
557 Holladay, J. E., Owen, J., Harmon, L., Burton, F., Palou-Rivera, I., Plaza, J., Handler, R., and Shonnard, D.:
558 Low-Carbon Aviation Fuel Through the Alcohol to Jet Pathway, in: *Biofuels for Aviation: Feedstocks,*
559 *Technology and Implementation*, Elsevier Inc., 109–150, <https://doi.org/10.1016/B978-0-12-804568-8.00006-8>,
560 2016.



- 561 Camacho, J., Liu, C., Gu, C., Lin, H., Huang, Z., Tang, Q., You, X., Saggese, C., Li, Y., Jung, H., Deng, L.,
562 Wlokas, I., and Wang, H.: Mobility size and mass of nascent soot particles in a benchmark premixed ethylene
563 flame, *Combust. Flame*, 162, 3810–3822, <https://doi.org/10.1016/j.combustflame.2015.07.018>, 2015.
- 564 Carbone, F., Gleason, K., and Gomez, A.: Soot research: Relevance and priorities by mid-century, in:
565 *Combustion Chemistry and the Carbon Neutral Future*, Elsevier Inc., 27–61, <https://doi.org/10.1016/B978-0-323-99213-8.00007-2>, 2023.
- 567 Cassee, F. R., Héroux, M. E., Gerlofs-Nijland, M. E., and Kelly, F. J.: Particulate matter beyond mass: Recent
568 health evidence on the role of fractions, chemical constituents and sources of emission, *Inhal. Toxicol.*, 25, 802–
569 812, <https://doi.org/10.3109/08958378.2013.850127>, 2013.
- 570 Cavalli, F., Viana, M., Yttri, K. E., Genberg, J., and Putaud, J.-P.: Toward a standardised thermal-optical
571 protocol for measuring atmospheric organic and elemental carbon: the EUSAAR protocol, *Atmos. Meas. Tech.*,
572 3, 79–89, <https://doi.org/10.5194/amt-3-79-2010>, 2010.
- 573 Ceruti, A., Marzocca, P., Liverani, A., and Bil, C.: Maintenance in aeronautics in an Industry 4.0 context: The
574 role of Augmented Reality and Additive Manufacturing, *J. Comput. Des. Eng.*, 6, 516–526,
575 <https://doi.org/10.1016/j.jcde.2019.02.001>, 2019.
- 576 Chong, S. T., Hassanaly, M., Koo, H., Mueller, M. E., Raman, V., and Geigle, K. P.: Large eddy simulation of
577 pressure and dilution-jet effects on soot formation in a model aircraft swirl combustor, *Combust. Flame*, 192,
578 452–472, <https://doi.org/10.1016/j.combustflame.2018.02.021>, 2018a.
- 579 Chong, S. T., Raman, V., Mueller, M. E., and Im, H. G.: The role of recirculation zones in soot formation in
580 aircraft combustors, *Proc. ASME Turbo Expo*, 4B-2018, 1–9, <https://doi.org/10.1115/GT2018-76217>, 2018b.
- 581 Chu, H., Qi, J., Feng, S., Dong, W., Hong, R., Qiu, B., and Han, W.: Soot formation in high-pressure
582 combustion: Status and challenges, *Fuel*, 345, 128236, <https://doi.org/10.1016/j.fuel.2023.128236>, 2023.
- 583 Commodo, M., D’Anna, A., De Falco, G., Larciprete, R., and Minutolo, P.: Illuminating the earliest stages of the
584 soot formation by photoemission and Raman spectroscopy, *Combust. Flame*, 181, 188–197,
585 <https://doi.org/10.1016/j.combustflame.2017.03.020>, 2017.
- 586 Commodo, M., Kaiser, K., De Falco, G., Minutolo, P., Schulz, F., D’Anna, A., and Gross, L.: On the early stages
587 of soot formation: Molecular structure elucidation by high-resolution atomic force microscopy, *Combust. Flame*,
588 205, 154–164, <https://doi.org/10.1016/j.combustflame.2019.03.042>, 2019.
- 589 Delhaye, D., Ouf, F. X., Ferry, D., Ortega, I. K., Penanhoat, O., Peillon, S., Salm, F., Vancassel, X., Focsa, C.,
590 Irimiea, C., Harivel, N., Perez, B., Quinton, E., Yon, J., and Gaffie, D.: The MERMOSE project:
591 Characterization of particulate matter emissions of a commercial aircraft engine, *J. Aerosol Sci.*, 105, 48–63,
592 <https://doi.org/10.1016/j.jaerosci.2016.11.018>, 2017.
- 593 Dobbins, R. A.: Soot inception temperature and the carbonization rate of precursor particles, *Combust. Flame*,
594 130, 204–214, [https://doi.org/10.1016/S0010-2180\(02\)00374-7](https://doi.org/10.1016/S0010-2180(02)00374-7), 2002.
- 595 Durdina, L., Brem, B. T., Abegglen, M., Lobo, P., Rindlisbacher, T., Thomson, K. A., Smallwood, G. J., Hagen,
596 D. E., Sierau, B., and Wang, J.: Determination of PM mass emissions from an aircraft turbine engine using
597 particle effective density, *Atmos. Environ.*, 99, 500–507, <https://doi.org/10.1016/j.atmosenv.2014.10.018>, 2014.
- 598 Durdina, L., Lobo, P., Trueblood, M. B., Black, E. A., Achterberg, S., Hagen, D. E., Brem, B. T., and Wang, J.:
599 Response of real-time black carbon mass instruments to mini-CAST soot, *Aerosol Sci. Technol.*, 50, 906–918,
600 <https://doi.org/10.1080/02786826.2016.1204423>, 2016.
- 601 Durdina, L., Brem, B. T., Setyan, A., Siegerist, F., Rindlisbacher, T., and Wang, J.: Assessment of Particle
602 Pollution from Jetliners: From Smoke Visibility to Nanoparticle Counting, *Environ. Sci. Technol.*, 51, 3534–
603 3541, <https://doi.org/10.1021/acs.est.6b05801>, 2017.
- 604 Durdina, L., Brem, B. T., Schönenberger, D., Siegerist, F., Anet, J. G., and Rindlisbacher, T.: Nonvolatile
605 Particulate Matter Emissions of a Business Jet Measured at Ground Level and Estimated for Cruising Altitudes,
606 *Environ. Sci. Technol.*, 53, 12865–12872, <https://doi.org/10.1021/acs.est.9b02513>, 2019.
- 607 Durdina, L., Brem, B. T., Elser, M., Sch, D., Siegerist, F., and Anet, J. G.: Reduction of Nonvolatile Particulate
608 Matter Emissions of a Commercial Turbofan Engine at the Ground Level from the Use of a Sustainable Aviation
609 Fuel Blend, *Environ. Sci. Technol.*, 55, 14576–14585, <https://doi.org/10.1021/acs.est.1c04744>, 2021.
- 610 Elser, M., Brem, B. T., Durdina, L., Schönenberger, D., Siegerist, F., Fischer, A., and Wang, J.: Chemical
611 composition and radiative properties of nascent particulate matter emitted by an aircraft turbofan burning
612 conventional and alternative fuels, *Atmos. Chem. Phys.*, 19, 6809–6820, <https://doi.org/10.5194/acp-19-6809-2019>



- 613 2019, 2019.
- 614 European Commission: Proposal for a Regulation of the European Parliament and of the council on ensuring a
615 level playing field for sustainable air transport, European Commission, 2021.
- 616 Foust, M. J., Thomsen, D., Stickles, R., Cooper, C., and Dodds, W.: Development of the GE aviation low
617 emissions TAPS combustor for next generation aircraft engines, 50th AIAA Aerosp. Sci. Meet. Incl. New
618 Horizons Forum Aerosp. Expo., 1–9, <https://doi.org/10.2514/6.2012-936>, 2012.
- 619 Franzelli, B., Tardelli, L., Stöhr, M., Geigle, K. P., and Domingo, P.: Assessment of LES of intermittent soot
620 production in an aero-engine model combustor using high-speed measurements, *Proc. Combust. Inst.*, 39, 4821–
621 4829, <https://doi.org/10.1016/j.proci.2022.09.060>, 2023.
- 622 Frenklach, M.: Reaction mechanism of soot formation in flames, *Phys. Chem. Chem. Phys.*, 4, 2028–2037,
623 <https://doi.org/10.1039/b110045a>, 2002.
- 624 Fric, T.: Low-emission combustor having perforated plate for lean direct injection, 1995.
- 625 Gao, K., Zhou, C. W., Meier, E. J. B., and Kanji, Z. A.: Laboratory studies of ice nucleation onto bare and
626 internally mixed soot-sulfuric acid particles, *Atmos. Chem. Phys.*, 22, 5331–5364, <https://doi.org/10.5194/acp-22-5331-2022>, 2022.
- 628 George, R. E., Nevitt, J. S., and Verssen, J. A.: Jet aircraft operations: Impact on the air environment, *J. Air
629 Pollut. Control Assoc.*, 22, 507–515, <https://doi.org/10.1080/00022470.1972.10469667>, 1972.
- 630 Gkantonas, S., Sirignano, M., Giusti, A., D’Anna, A., and Mastorakos, E.: Comprehensive soot particle size
631 distribution modelling of a model Rich-Quench-Lean burner, *Fuel*, 270, 117483,
632 <https://doi.org/10.1016/j.fuel.2020.117483>, 2020.
- 633 Goudeli, E., Eggersdorfer, M. L., and Pratsinis, S. E.: Coagulation-agglomeration of fractal-like particles:
634 Structure and self-preserving size distribution, *Langmuir*, 31, 1320–1327, <https://doi.org/10.1021/la504296z>,
635 2015.
- 636 Han, J., Elgowainy, A., Cai, H., and Wang, M. Q.: Life-cycle analysis of bio-based aviation fuels, *Bioresour.
637 Technol.*, 150, 447–456, <https://doi.org/10.1016/j.biortech.2013.07.153>, 2013.
- 638 El Helou, I., Skiba, A. W., and Mastorakos, E.: Experimental Investigation of Soot Production and Oxidation in
639 a Lab-Scale Rich–Quench–Lean (RQL) Burner, *Flow, Turbul. Combust.*, 106, 1019–1041,
640 <https://doi.org/10.1007/s10494-020-00113-5>, 2021.
- 641 ICAO: Annex 16 to the convention on international civil aviation: environmental protection, Vol. II - aircraft
642 engine emissions, Montreal, CA, 4th ed. pp., 2017.
- 643 ICAO: Sustainable Aviation Fuels Guide, 1–66 pp., 2018.
- 644 ICAO Aircraft Engine Emissions Databank: [https://www.easa.europa.eu/en/domains/environment/icao-aircraft-
645 engine-emissions-databank](https://www.easa.europa.eu/en/domains/environment/icao-aircraft-engine-emissions-databank), last access: 8 August 2023.
- 646 Johnson, T. J., Olfert, J. S., Symonds, J. P. R., Johnson, M., Rindlisbacher, T., Swanson, J. J., Boies, A. M.,
647 Thomson, K., Smallwood, G., Walters, D., Sevcenco, Y., Crayford, A., Dastanpour, R., Rogak, S. N., Durdina,
648 L., Bahk, Y. K., Brem, B., and Wang, J.: Effective Density and Mass-Mobility Exponent of Aircraft Turbine
649 Particulate Matter, *J. Propuls. Power*, 31, 573–580, <https://doi.org/10.2514/1.B35367>, 2015.
- 650 Kärcher, B.: Formation and radiative forcing of contrail cirrus, *Nat. Commun.*, 9, 1824,
651 <https://doi.org/10.1038/s41467-018-04068-0>, 2018.
- 652 Kelesidis, G. A. and Goudeli, E.: Self-preserving size distribution and collision frequency of flame-made
653 nanoparticles in the transition regime, *Proc. Combust. Inst.*, 38, 1233–1240,
654 <https://doi.org/10.1016/j.proci.2020.07.147>, 2021.
- 655 Kelesidis, G. A., Goudeli, E., and Pratsinis, S. E.: Flame synthesis of functional nanostructured materials and
656 devices: Surface growth and aggregation, *Proc. Combust. Inst.*, 36, 29–50,
657 <https://doi.org/10.1016/j.proci.2016.08.078>, 2017a.
- 658 Kelesidis, G. A., Goudeli, E., and Pratsinis, S. E.: Morphology and mobility diameter of carbonaceous aerosols
659 during agglomeration and surface growth, *Carbon*, 121, 527–535, <https://doi.org/10.1016/j.carbon.2017.06.004>,
660 2017b.
- 661 Kelesidis, G. A., Kholghy, M. R., Zuercher, J., Robertz, J., Allemann, M., Duric, A., and Pratsinis, S. E.: Light
662 scattering from nanoparticle agglomerates, *Powder Technol.*, 365, 52–59,
663 <https://doi.org/10.1016/j.powtec.2019.02.003>, 2020.



- 664 Kelesidis, G. A., Bruun, C. A., and Pratsinis, S. E.: The impact of organic carbon on soot light absorption,
665 Carbon, 172, 742–749, <https://doi.org/10.1016/j.carbon.2020.10.032>, 2021.
- 666 Kelesidis, G. A., Neubauer, D., Fan, L. S., Lohmann, U., and Pratsinis, S. E.: Enhanced Light Absorption and
667 Radiative Forcing by Black Carbon Agglomerates, Environ. Sci. Technol., 56, 8610–8618,
668 <https://doi.org/10.1021/acs.est.2c00428>, 2022.
- 669 Kelesidis, G. A., Benz, S., and Pratsinis, S. E.: Process design for carbon black size and morphology, Carbon,
670 213, 118255, <https://doi.org/10.1016/j.carbon.2023.118255>, 2023a.
- 671 Kelesidis, G. A., Nagarkar, A., Trivanovic, U., and Pratsinis, S. E.: Toward Elimination of Soot Emissions from
672 Jet Fuel Combustion, Environ. Sci. Technol., 57, 10276–10283, <https://doi.org/10.1021/acs.est.3c01048>, 2023b.
- 673 Kholghy, M., Saffaripour, M., Yip, C., and Thomson, M. J.: The evolution of soot morphology in a laminar
674 coflow diffusion flame of a surrogate for Jet A-1, Combust. Flame, 160, 2119–2130,
675 <https://doi.org/10.1016/j.combustflame.2013.04.008>, 2013.
- 676 Kim, D., Ekoto, I., Colban, W. F., and Miles, P. C.: In-cylinder CO and UHC imaging in a light-duty diesel
677 engine during PPCI low-temperature combustion, SAE Int. J. Fuels Lubr., 1, 933–956,
678 <https://doi.org/10.4271/2008-01-1602>, 2009.
- 679 Koudis, G. S., Hu, S. J., Majumdar, A., Jones, R., and Stettler, M. E. J.: Airport emissions reductions from
680 reduced thrust takeoff operations, Transp. Res. Part D Transp. Environ., 52, 15–28,
681 <https://doi.org/10.1016/j.trd.2017.02.004>, 2017.
- 682 Lee, D. S., Fahey, D. W., Skowron, A., Allen, M. R., Burkhardt, U., Chen, Q., Doherty, S. J., Freeman, S.,
683 Forster, P. M., Fuglestvedt, J., Gettelman, A., De León, R. R., Lim, L. L., Lund, M. T., Millar, R. J., Owen, B.,
684 Penner, J. E., Pitari, G., Prather, M. J., Sausen, R., and Wilcox, L. J.: The contribution of global aviation to
685 anthropogenic climate forcing for 2000 to 2018, Atmos. Environ., 244,
686 <https://doi.org/10.1016/j.atmosenv.2020.117834>, 2021.
- 687 Liati, A., Brem, B. T., Durdina, L., Vögltl, M., Dasilva, Y. A. R., Eggenschwiler, P. D., and Wang, J.: Electron
688 microscopic study of soot particulate matter emissions from aircraft turbine engines, Environ. Sci. Technol., 48,
689 10975–10983, <https://doi.org/10.1021/es501809b>, 2014.
- 690 Liati, A., Schreiber, D., Alpert, P. A., Liao, Y., Brem, B. T., Corral Arroyo, P., Hu, J., Jonsdottir, H. R.,
691 Ammann, M., and Dimopoulos Eggenschwiler, P.: Aircraft soot from conventional fuels and biofuels during
692 ground idle and climb-out conditions: Electron microscopy and X-ray micro-spectroscopy, Environ. Pollut., 247,
693 658–667, <https://doi.org/10.1016/j.envpol.2019.01.078>, 2019.
- 694 Liu, Y., Sun, X., Sethi, V., Nalianda, D., Li, Y. G., and Wang, L.: Review of modern low emissions combustion
695 technologies for aero gas turbine engines, Prog. Aerosp. Sci., 94, 12–45,
696 <https://doi.org/10.1016/j.paerosci.2017.08.001>, 2017.
- 697 Lobo, P., Christie, S., Khandelwal, B., Blakey, S. G., and Raper, D. W.: Evaluation of Non-volatile Particulate
698 Matter Emission Characteristics of an Aircraft Auxiliary Power Unit with Varying Alternative Jet Fuel Blend
699 Ratios, Energy and Fuels, 29, 7705–7711, <https://doi.org/10.1021/acs.energyfuels.5b01758>, 2015a.
- 700 Lobo, P., Durdina, L., Smallwood, G. J., Rindlisbacher, T., Siegerist, F., Black, E. A., Yu, Z., Mensah, A. A.,
701 Hagen, D. E., Miake-Lye, R. C., Thomman, K. A., Brem, B. T., Corbin, J. C., Abegglen, M., Sierau, B.,
702 Whitefield, P. D., and Wang, J.: Measurement of aircraft engine non-volatile PM emissions: Results of the
703 Aviation-Particle Regulatory Instrumentation Demonstration Experiment (A-PRIDE) 4 campaign, Aerosol Sci.
704 Technol., 49, 472–484, <https://doi.org/10.1080/02786826.2015.1047012>, 2015b.
- 705 Marcolli, C., Mahrt, F., and Kärcher, B.: Soot PCF: Pore condensation and freezing framework for soot
706 aggregates, Atmos. Chem. Phys., 21, 7791–7843, <https://doi.org/10.5194/acp-21-7791-2021>, 2021.
- 707 Marhaba, I., Ferry, D., Laffon, C., Regier, T. Z., Ouf, F., and Parent, P.: Aircraft and MiniCAST soot at the
708 nanoscale, Combust. Flame, 204, 278–289, <https://doi.org/10.1016/j.combustflame.2019.03.018>, 2019.
- 709 Masiol, M. and Harrison, R. M.: Aircraft engine exhaust emissions and other airport-related contributions to
710 ambient air pollution: A review, Atmos. Environ., 95, 409–455, <https://doi.org/10.1016/j.atmosenv.2014.05.070>,
711 2014.
- 712 Messerer, A., Niessner, R., and Pöschl, U.: Comprehensive kinetic characterization of the oxidation and
713 gasification of model and real diesel soot by nitrogen oxides and oxygen under engine exhaust conditions:
714 Measurement, Langmuir-Hinshelwood, and Arrhenius parameters, Carbon, 44, 307–324,
715 <https://doi.org/10.1016/j.carbon.2005.07.017>, 2006.



- 716 Miniero, L., Pandey, K., De Falco, G., D'Anna, A., and Noiray, N.: Soot-free and low-NO combustion of Jet A-
717 1 in a lean azimuthal flame (LEAF) combustor with hydrogen injection, *Proc. Combust. Inst.*, 39, 4309–4318,
718 <https://doi.org/10.1016/j.proci.2022.08.006>, 2023.
- 719 Mongia, H. C.: GE aviation low emissions combustion technology evolution, *SAE Tech. Pap.*, 776–790,
720 <https://doi.org/10.4271/2007-01-3924>, 2007.
- 721 Montzka, S. A., Dlugokencky, E. J., and Butler, J. H.: Non-CO₂ greenhouse gases and climate change, *Nature*,
722 476, 43–50, <https://doi.org/10.1038/nature10322>, 2011.
- 723 Moore, R. H., Thornhill, K. L., Weinzierl, B., Sauer, D., D'Ascoli, E., Kim, J., Lichtenstern, M., Scheibe, M.,
724 Beaton, B., Beyersdorf, A. J., Barrick, J., Bulzan, D., Corr, C. A., Crosbie, E., Jurkat, T., Martin, R., Riddick, D.,
725 Shook, M., Slover, G., Voigt, C., White, R., Winstead, E., Yasky, R., Ziemba, L. D., Brown, A., Schlager, H.,
726 and Anderson, B. E.: Biofuel blending reduces particle emissions from aircraft engines at cruise conditions,
727 *Nature*, 543, 411–415, <https://doi.org/10.1038/nature21420>, 2017.
- 728 National Academies of Sciences Engineering and Medicine: Options for Reducing Lead Emissions from Piston-
729 Engine Aircraft, <https://doi.org/10.17226/26050>, 2021.
- 730 Nguyen, T. H., Tri Nguyen, P., and Garnier, F.: Evaluation of the relationship between the aerothermodynamic
731 process and operational parameters in the high-pressure turbine of an aircraft engine, *Aerosp. Sci. Technol.*, 86,
732 93–105, <https://doi.org/10.1016/j.ast.2019.01.011>, 2019.
- 733 Niranjana, R. and Thakur, A. K.: The toxicological mechanisms of environmental soot (black carbon) and carbon
734 black: Focus on Oxidative stress and inflammatory pathways, *Front. Immunol.*, 8, 763,
735 <https://doi.org/10.3389/fimmu.2017.00763>, 2017.
- 736 Novic, A. S., Troth, D. L. L., Notardonato, J., Novick, A. S., Troth, D. L. L., and Notardonato, J.: Multifuel
737 Evaluation of Rich/Quench/Lean Combustor, in: *Proceedings of the ASME 1983 International Gas Turbine
738 Conference and Exhibit*, 1–8, <https://doi.org/10.1115/83-GT-140>, 1983.
- 739 Oliveira, P. M. De, Fredrich, D., Falco, G. De, Helou, I. El, Anna, A. D., Giusti, A., and Mastorakos, E.: Soot-
740 Free Low-NO_x Aeronautical Combustor Concept: The Lean Azimuthal Flame for Kerosene Sprays, *Energy and
741 Fuels*, 35, 7092–7106, <https://doi.org/10.1021/acs.energyfuels.0c03860>, 2021.
- 742 Parent, P., Laffon, C., Marhaba, I., Ferry, D., Regier, T. Z., Ortega, I. K., Chazallon, B., Carpentier, Y., and
743 Focsa, C.: Nanoscale characterization of aircraft soot: A high-resolution transmission electron microscopy ,
744 Raman spectroscopy , X-ray photoelectron and near-edge X-ray absorption spectroscopy study, *Carbon*, 101,
745 86–100, <https://doi.org/10.1016/j.carbon.2016.01.040>, 2016.
- 746 Prabhakar, N., Heyerdahl, L., Jha, A., and Karbowski, D.: Energy Impacts of Electric Aircraft: An Overview,
747 *AIAA Aviat. 2022 Forum*, <https://doi.org/10.2514/6.2022-4119>, 2022.
- 748 Rissler, J., Swietlicki, E., Bengtsson, A., Boman, C., Pagels, J., Sandström, T., Blomberg, A., and Löndahl, J.:
749 Experimental determination of deposition of diesel exhaust particles in the human respiratory tract, *J. Aerosol
750 Sci.*, 48, 18–33, <https://doi.org/10.1016/j.jaerosci.2012.01.005>, 2012.
- 751 Rizk, N. K. and Mongia, H. C.: Ultra-Low NO_x Rich-Lean Combustion, *Am. Soc. Mech. Eng.*, 1990.
- 752 Saffaripour, M., Tay, L. L., Thomson, K. A., Smallwood, G. J., Brem, B. T., Durdina, L., and Johnson, M.:
753 Raman spectroscopy and TEM characterization of solid particulate matter emitted from soot generators and
754 aircraft turbine engines, *Aerosol Sci. Technol.*, 51, 518–531, <https://doi.org/10.1080/02786826.2016.1274368>,
755 2017.
- 756 Schäfer, A. W., Barrett, S. R. H., Doyme, K., Dray, L. M., Gnadt, A. R., Self, R., O'Sullivan, A., Synodinos, A.
757 P., and Torija, A. J.: Technological, economic and environmental prospects of all-electric aircraft, *Nat. Energy*,
758 4, 160–166, <https://doi.org/10.1038/s41560-018-0294-x>, 2019.
- 759 Schäppi, R., Rutz, D., Dähler, F., Muroyama, A., Haueter, P., Lilliestam, J., Patt, A., Furler, P., and Steinfeld,
760 A.: Drop-in fuels from sunlight and air, *Nature*, 601, 63–68, <https://doi.org/10.1038/s41586-021-04174-y>, 2022.
- 761 Schripp, T., Grein, T., Zinsmeister, J., Oßwald, P., Köhler, M., Müller-Langer, F., Hauschild, S., Marquardt, C.,
762 Scheuermann, S., Zschocke, A., and Posselt, D.: Technical application of a ternary alternative jet fuel blend –
763 Chemical characterization and impact on jet engine particle emission, *Fuel*, 288,
764 <https://doi.org/10.1016/j.fuel.2020.119606>, 2021.
- 765 Schulz, F., Commodo, M., Kaiser, K., De Falco, G., Minutolo, P., Meyer, G., D'Anna, A., and Gross, L.:
766 Insights into incipient soot formation by atomic force microscopy, *Proc. Combust. Inst.*, 37, 885–892,
767 <https://doi.org/10.1016/j.proci.2018.06.100>, 2019.



- 768 Sharma, A., Mukut, K. M., Roy, S. P., and Goudeli, E.: The coalescence of incipient soot clusters, *Carbon*, 180,
769 215–225, <https://doi.org/10.1016/j.carbon.2021.04.065>, 2021.
- 770 Staples, M. D., Malina, R., Suresh, P., Hileman, J. I., and Barrett, S. R. H.: Aviation CO₂ emissions reductions
771 from the use of alternative jet fuels, *Energy Policy*, 114, 342–354, <https://doi.org/10.1016/j.enpol.2017.12.007>,
772 2018.
- 773 Stettler, M. E. J., Boies, A. M., Petzold, A., and Barrett, S. R. H.: Global civil aviation black carbon emissions,
774 *Environ. Sci. Technol.*, 47, 10397–10404, <https://doi.org/10.1021/es401356v>, 2013.
- 775 Stuber, N., Forster, P., Rädcl, G., and Shine, K.: The importance of the diurnal and annual cycle of air traffic for
776 contrail radiative forcing, *Nature*, 441, 864–867, <https://doi.org/10.1038/nature04877>, 2006.
- 777 Teoh, R., Schumann, U., Majumdar, A., and Stettler, M. E. J.: Mitigating the Climate Forcing of Aircraft
778 Contrails by Small-Scale Diversions and Technology Adoption, *Environ. Sci. Technol.*, 54, 2941–2950,
779 <https://doi.org/10.1021/acs.est.9b05608>, 2020.
- 780 Teoh, R., Schumann, U., Gryspeerdt, E., Shapiro, M., Molloy, J., Koudis, G., Voigt, C., and Stettler, M. E. J.:
781 Aviation contrail climate effects in the North Atlantic from 2016 to 2021, *Atmos. Chem. Phys.*, 22, 10919–
782 10935, <https://doi.org/10.5194/acp-22-10919-2022>, 2022a.
- 783 Teoh, R., Schumann, U., Voigt, C., Schripp, T., Shapiro, M., Engberg, Z., Molloy, J., Koudis, G., and Stettler,
784 M. E. J.: Targeted Use of Sustainable Aviation Fuel to Maximize Climate Benefits, *Environ. Sci. Technol.*, 56,
785 17246–17255, <https://doi.org/10.1021/acs.est.2c05781>, 2022b.
- 786 Trivanovic, U., Kelesidis, G. A., and Pratsinis, S. E.: High-throughput generation of aircraft-like soot, *Aerosol*
787 *Sci. Technol.*, 56, 732–743, <https://doi.org/10.1080/02786826.2022.2070055>, 2022.
- 788 Trivanovic, U., Pereira Martins, M., Benz, S., Kelesidis, G. A., and Pratsinis, S. E.: Dynamics of soot surface
789 growth and agglomeration by enclosed spray combustion of jet fuel, *Fuel*, 342, 127864, 2023.
- 790 Undavalli, V., Gbadamosi Olatunde, O. B., Boylu, R., Wei, C., Haeker, J., Hamilton, J., and Khandelwal, B.:
791 Recent advancements in sustainable aviation fuels, *Prog. Aerosp. Sci.*, 136, 100876,
792 <https://doi.org/10.1016/j.paerosci.2022.100876>, 2023.
- 793 Vander Wal, R. L., Bryg, V. M., and Hays, M. D.: Fingerprinting soot (towards source identification): Physical
794 structure and chemical composition, *J. Aerosol Sci.*, 41, 108–117, <https://doi.org/10.1016/j.jaerosci.2009.08.008>,
795 2010.
- 796 Vander Wal, R. L., Bryg, V. M., and Huang, C. H.: Aircraft engine particulate matter: Macro- micro- and
797 nanostructure by HRTEM and chemistry by XPS, *Combust. Flame*, 161, 602–611,
798 <https://doi.org/10.1016/j.combustflame.2013.09.003>, 2014.
- 799 Wang, H.: Formation of nascent soot and other condensed-phase materials in flames, *Proc. Combust. Inst.*, 33,
800 41–67, <https://doi.org/10.1016/j.proci.2010.09.009>, 2011.
- 801 Xue, X., Hui, X., Vannorsdall, P., Singh, P., and Sung, C. J.: The blending effect on the sooting tendencies of
802 alternative/conventional jet fuel blends in non-premixed flames, *Fuel*, 237, 648–657,
803 <https://doi.org/10.1016/j.fuel.2018.09.157>, 2019.
- 804 Yang, Y., Bohman, A. L., and Santoro, R. J.: A study of jet fuel sooting tendency using the threshold sooting
805 index (TSI) model, *Combust. Flame*, 149, 191–205, <https://doi.org/10.1016/j.combustflame.2006.11.007>, 2007.
- 806